Signal Processing 180 (2021) 107872

Contents lists available at ScienceDirect

Signal Processing

journal homepage: www.elsevier.com/locate/sigpro

Structured sparse array design exploiting two uniform subarrays for DOA estimation on moving platform

Guodong Qin[a,*], Moeness G. Amin[b]

[a] School of Electronic Engineering, Xidian University, Xian, Shaanxi 710071, China
[b] Center for Advanced Communications, Villanova University, Villanova, PA 19085, USA

ARTICLE INFO

Article history:
Received 17 July 2020
Revised 15 October 2020
Accepted 2 November 2020
Available online 6 November 2020

Keywords:
DOA estimation
Sparse array
Array design
Difference co-array
Array motion

ABSTRACT

Array motion can efficiently enhance the achievable number of degrees-of-freedom (DOFs) by the virtue of filling the neighboring holes of each lag in the difference co-array of a linear sparse array. In this paper, a new structured sparse array design exploiting two uniform subarrays on a moving platform is proposed for direction-of arrival (DOA) estimation problems. The proposed array design yields a fully filled co-array. It compresses sensor spacing of one subarray to three times the unit sensor spacing while dilating that of the other subarray. The numbers of sensors in the two subarrays are chosen as arbitrary integers without the limitation of coprimality. The conditions on the array parameters to achieve full augmentability under array motion are provided. Closed-form expressions of maximum DOFs in the difference co-array of the synthetic array, which comprises the sensor positions before and after motion, are delineated. The non-coprimality of the sensor numbers is analyzed when the two subarrays are aligned at the reference sensor, and shown to offer higher DOFs than the coprimality. Numerical results of DOA estimation using the proposed array design are provided for performance comparison and validations of analysis.

1. Introduction

Direction-of arrival (DOA) estimation exploiting sparse arrays can offer a high number of degrees-of-freedom (DOFs) with relatively low cost, hence it is widely utilized in communications, radar, sonar, and satellite navigation [1–21]. The coprime array [4] and the nested array [5] are commonly used examples for structured sparse array design, where two uniform subarrays are employed to form a sparse array. Generally, by using sparse array configurations, $O(N^2)$ uncorrelated far-field narrowband sources can be estimated from the data collected by $O(N)$ sensors [11].

The difference co-array arises in passive sensing where the DOA estimation involves the spatial correlation lags, in lieu of the sensor data, along with the source power and steering vectors. Carefully designed sparse arrays enable the creation of large virtual arrays and, as such, lead to improved DOA estimation. In general, depending on the sensor positions, some lags could be missing while others could be redundantly computed. From this perspective, different sparse array designs have been introduced, including minimum redundant arrays (MRAs) [22] and minimum hole arrays (MHAs) [23]. Sparse array design typically defines the sensor spacings and the relative distance of the two uniform subarrays constituting the sparse array, as in the case of the generalized coprime array [11]. More recently, the shifted coprime array configuration was proposed in [24] to secure more consecutive lags with a smaller array aperture compared with the generalized coprime array with displaced subarrays.

All the above cases assume the arrays to be mounted on fixed platforms or, more generally, ignore the motion of the sensor platform. With array motion, a synthetic array can be formed by combining the original sparse array and its shifted version under the assumption of slowly time-varying signal environment. In this respect, a moving coprime array was proposed in [25] to provide a hole-free co-array for a strict stationary signal environment and for the case of larger array aperture. The array moving distance was defined as $N/2$ half-wavelength for two subarrays of M and N sensors. In our previous works [26–29], the motion distance was confined to half-wavelength, which is much less restrictive than the condition imposed in [25]. Different sparse arrays on moving platforms, including the coprime array, nested array, MRAs, MHAs and uniform sparse array, were discussed and analyzed in [26]. It was shown that the difference co-array of the synthetic array is the combination of the difference co-array of the original array and its unit lag shifted versions along and opposite to the direction of motion. In [28], a dilated nested array was proposed to obtain a hole-free co-array by expanding the sensor spacings of the two

* Corresponding author.
E-mail addresses: gdqin@mail.xidian.edu.cn (G. Qin), moeness.amin@villanova.edu (M.G. Amin).

https://doi.org/10.1016/j.sigpro.2020.107872
0165-1684/

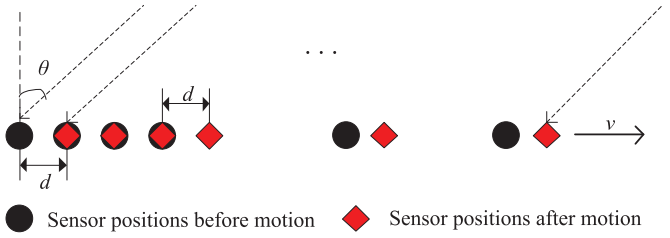

Fig. 1. DOA Estimation exploiting a moving sparse array.

subarrays. It is noted however that, even with array translational motion, the resulting synthetic array may not be fully augmented, that is, the corresponding difference co-arrays can still be sparse.

In this paper, we propose a novel sparse array design to provide a hole-free difference co-array with merely a half-wavelength array motion. The proposed array is divided into three categories according to the distance between the two subarrays. Fundamentally, we consider two subarrays, named as subarray1 and subarray2, consisting of M and N sensors, respectively. The sensor spacing of subarray1 is taken as three times the unit spacing, and that of subarray2 is dilated by an integer multiple of M unit spacing. Unlike the coprime array, the numbers of the two subarrays M, N are just arbitrary integers. We drive the expressions describing the subarray configurations leading to a fully filled co-array. The optimal distance between two subarrays and the values of M, N are determined under the criterion of maximum DOFs. The advantages of relaxing coprimality of M, N are discussed and illustrated by simulation examples. The latter implement the co-array MUSIC algorithm [5,13] for DOA estimation.

The remainder of the paper is organized as follows. The moving sparse array synthesis process and DOA estimations using co-array MUSIC are summarized in Section 1. In Section 2, the difference co-array associated with a moving platform is reviewed. Section 4 describes the proposed array structure along with the conditions on the different parameters leading to a fully filled co-array. In this section, the optimal values of M and N as well as the distance between the two subarrays are determined based on maximum DOFs. In Section 5, the performance of the proposed array is evaluated through simulations. Section 6 concludes the paper.

Notations: We use lower-case (upper-case) bold characters to denote vectors (matrices). In particular, $\mathbf{I}_N$ denotes the $N\times N$ identity matrix. $(\cdot)^*$ implies complex conjugation, whereas $(\cdot)^T$ and $(\cdot)^H$ respectively denote the transpose and conjugate transpose of a matrix or a vector. $vec(\cdot)$ denotes the vectorization operator that turns a matrix into a vector by stacking all columns on top of the another. $E(\cdot)$ is the statistical expectation operator and $\otimes$ denotes the Kronecker product. $\mathbb{S}$ denotes the sets of integers, and $\mathbb{C}$ denotes the sets of complex values. $diag\{\mathbf{x}\}$ represents a diagonal matrix that uses the elements of $\mathbf{x}$ as its diagonal elements. $\cup$ denotes the union operation.

2. Problem formulation

2.1. Signal model

We consider a one-dimension (1-D) sparse array with K sensors moving at a constant velocity v. The schematic is illustrated in Fig. 1, where the black circles and red rhombus represent the sensor positions of the original and the shifted arrays, respectively. The minimum inter-element spacing is denoted as $d = \lambda/2$, where λ represents the wavelength. All the sensor positions are integer multiplication of d. Denote $\mathbf{D} = [d_l, \ldots, d_K]^T$ as the array sensor positions, where d_k, $k = 1, 2, \ldots, K$ is the position of the kth sensor. The first sensor is used as a reference, i.e., $d_1 = 0$. The received signals from Q uncorrelated far-field narrowband sources are described as $s_q(t)$, $t = T_s, 2T_s, \ldots, L_sT_s$, for $q = 1, \ldots, Q$, where T_s and L_s, respectively, represent the sampling interval and the number of snapshots. The arrival angle of the qth source is denoted as θ_q. Because of the assumed short translation motion of the array, the directions of the sources with respect to the sensor array can be considered unchanged during the short processing time. The output of the receive array, at time t, is expressed as

$$\begin{aligned}\mathbf{x}(\mathbf{t}) &= \sum_{\mathbf{q=1}}^{\mathbf{Q}} \mathbf{s_q(t)} \exp(-\mathbf{j2\pi vt}\sin(\theta_\mathbf{q})/\lambda)\mathbf{a}(\theta_\mathbf{q}) + \boldsymbol{\varepsilon}(\mathbf{t}) \\ &= \mathbf{A}\mathbf{s}(t) + \boldsymbol{\varepsilon}(t),\end{aligned} \tag{1}$$

where $\mathbf{a}(\theta_q) = [1, \exp(-j2\pi \frac{d_2 \sin(\theta_q)}{\lambda}), \ldots, \exp(-j2\pi \frac{d_K \sin(\theta_q)}{\lambda})]^T$ represents the steering vector corresponding to θ_q. $\mathbf{A} = [\mathbf{a}(\theta_1), \ldots, \mathbf{a}(\theta_Q)] \in \mathbb{C}^{K\times Q}$ is the array manifold matrix. In the above equation, $\mathbf{s}(t) = [s_1(t)\exp(-j2\pi \frac{vt\sin(\theta_1)}{\lambda}), \ldots, s_Q(t)\exp(-j2\pi \frac{vt\sin(\theta_Q)}{\lambda})]^T$ is signal vector and $\boldsymbol{\varepsilon}(t) \in \mathbb{C}^{K\times 1}$ is zero-mean additive white complex Gaussian noise vector with covariance matrix $\sigma_{\boldsymbol{\varepsilon}}^2\mathbf{I}_K$. At time $t+\tau$, the output of the receive array becomes

$$\begin{aligned}\mathbf{x}(t+\tau) &= \sum_{q=1}^{Q} s_q(t+\tau)\exp(-j2\pi vt\sin(\theta_q)/\lambda) \\ &\quad \cdot \exp(-j2\pi v\tau\sin(\theta_q)/\lambda)\mathbf{a}(\theta_q) + \boldsymbol{\varepsilon}(t+\tau) \\ &= \mathbf{B}\mathbf{s}(t+\tau) + \boldsymbol{\varepsilon}(t+\tau),\end{aligned} \tag{2}$$

where $\mathbf{B} = [\mathbf{b}(\theta_1), \ldots, \mathbf{b}(\theta_Q)] \in \mathbb{C}^{K\times Q}$, with

$$\begin{aligned}\mathbf{b}(\theta_q) &= \exp(-j2\pi v\tau\sin(\theta_q)/\lambda)\mathbf{a}(\theta_q) \\ &= [\exp(-j2\pi v\tau\sin(\theta_q)/\lambda), \\ &\quad \exp(-j2\pi(v\tau + d_2)\sin(\theta_q)/\lambda), \ldots, \\ &\quad \exp(-j2\pi(v\tau + d_L)\sin(\theta_q)/\lambda)]^T,\end{aligned} \tag{3}$$

and the signal vector at time $t+\tau$ is $\mathbf{s}(t+\tau) = [s_1(t+\tau)\exp(-j2\pi \frac{vt\sin(\theta_1)}{\lambda}), \ldots, s_Q(t+\tau)\exp(-j2\pi \frac{vt\sin(\theta_Q)}{\lambda})]^T$. In addition, $\boldsymbol{\varepsilon}(t+\tau)$ is the noise vector at time $t+\tau$. We assume that $\boldsymbol{\varepsilon}(t)$ and $\boldsymbol{\varepsilon}(t+\tau)$ are uncorrelated.

For narrowband signals with carrier frequency f, $s_q(t+\tau) = s_q(t)\exp(j2\pi f\tau)$. Accordingly, (2) can be rewritten as

$$\mathbf{x}(t+\tau) = \exp(j2\pi f\tau)\mathbf{B}\mathbf{s}(t) + \boldsymbol{\varepsilon}(t+\tau). \tag{4}$$

By choosing $v\tau = d = \lambda/2$, the steering vector at time $t+\tau$ becomes

$$\begin{aligned}\mathbf{b}(\theta_q) &= [\exp(-j\pi\sin(\theta_q)), \exp(-j\pi(1 + d_2/d)\sin(\theta_q)), \ldots, \\ &\quad \exp(-j\pi(1 + d_L/d)\sin(\theta_q))]^T.\end{aligned} \tag{5}$$

Multiplying $\mathbf{x}(t+\tau)$ by the phase correction factor $\exp(-j2\pi f\tau)$, we obtain the phase synchronized received signal vector as [30]

$$\tilde{\mathbf{x}}(t+\tau) = \mathbf{x}(t+\tau)\exp(-j2\pi f\tau) = \mathbf{B}\mathbf{s}(t) + \tilde{\boldsymbol{\varepsilon}}(t+\tau), \tag{6}$$

where $\tilde{\boldsymbol{\varepsilon}}(t+\tau) = \exp(-j2\pi f\tau)\boldsymbol{\varepsilon}(t+\tau)$. Combining Eqs. (1) and (6) yields,

$$\mathbf{y}(t) = \begin{bmatrix}\mathbf{x}(t) \\ \tilde{\mathbf{x}}(t+\tau)\end{bmatrix} = \mathbf{A}_s\mathbf{s}(t) + \boldsymbol{\varepsilon}_s(t). \tag{7}$$

where $\mathbf{A}_s = [\mathbf{a}_s(\theta_1), \ldots, \mathbf{a}_s(\theta_Q)] \in \mathbb{C}^{L_c\times Q}$, $\mathbf{a}_s(\theta_q) = [\mathbf{a}^T(\theta_q), \mathbf{b}^T(\theta_q)]^T \in \mathbb{C}^{L_c\times 1}$, with $L_c \le 2K$ denoting the number of the sensors in $\mathbf{y}(t)$, and $\boldsymbol{\varepsilon}_s(t) = \left[\boldsymbol{\varepsilon}^T(t), \tilde{\boldsymbol{\varepsilon}}^T(t+\tau)\right]^T$.

2.2. DOA estimation

DOA estimation using sparse array can be obtained based on sparse signal reconstruction techniques [6,31–33] or co-array MUSIC [5,13]. We apply the latter to a hole-free difference co-array, as discussed below.

The covariance matrix of $\mathbf{y}(t)$ is defined as

$$\mathbf{R}_{\mathbf{y}} = E[\mathbf{y}(t)\mathbf{y}^H(t)] = \mathbf{A}_s\mathbf{R}_{\mathbf{s}}\mathbf{A}_s{}^H + \sigma_{\boldsymbol{\epsilon}}^2\mathbf{I}_{L_c}, \tag{8}$$

where $\mathbf{R}_{\mathbf{s}} = E[\mathbf{s}(t)\mathbf{s}^H(t)] = \text{diag}([\sigma_1^2, \ldots, \sigma_Q^2])$ is the source covariance matrix, with σ_q^2 denoting the input power of the qth source signal. In practice, the covariance matrix $\mathbf{R}_{\mathbf{y}}$ is estimated from L_s snapshots, i.e.,

$$\tilde{\mathbf{R}}_{\mathbf{y}} = \frac{1}{L_s}\sum_{l_s=1}^{L_s}\mathbf{y}(t)\mathbf{y}^H(t). \tag{9}$$

Vectorizing $\tilde{\mathbf{R}}_{\mathbf{y}}$ in (9) yields,

$$\mathbf{z} = vec(\tilde{\mathbf{R}}_{\mathbf{y}}) = \tilde{\mathbf{A}}\mathbf{p}_{\mathbf{s}} + \sigma_{\epsilon}^2\tilde{\mathbf{I}}, \tag{10}$$

where $\tilde{\mathbf{A}} = [\tilde{\mathbf{a}}_s(\theta_1), \ldots, \tilde{\mathbf{a}}_s(\theta_Q)]$, $\tilde{\mathbf{a}}_s(\theta_q) = \mathbf{a}_s^*(\theta_q) \bigotimes \mathbf{a}_s(\theta_q)$, $\mathbf{p}_s = [\sigma_1^2, \ldots, \sigma_Q^2]^T$, $\tilde{\mathbf{I}} = vec(\mathbf{I}_{L_c})$. The spatial smoothing matrix $\tilde{\mathbf{R}}_{ss}$ is given by [5,11]

$$\tilde{\mathbf{R}}_{ss} = \frac{1}{L_{ss}}\sum_{i=1}^{L_{ss}}\mathbf{R}_i. \tag{11}$$

where $L_{ss} = (L_{\text{ULA}} + 1)/2$ with L_{ULA} denoting the number of contiguous lags in the difference co-array of $\mathbf{y}(t)$. $\mathbf{R}_i$ is the convariance matrix of the ith smoothing subarray.

Alternatively, $\tilde{\mathbf{R}}_{ss}$ can be computed from the expression $\tilde{\mathbf{R}}_{ss} = \tilde{\mathbf{R}}^2/L_{ss}$ [13], where $\tilde{\mathbf{R}}$ is a Toeplitz matrix [13],

$$\tilde{\mathbf{R}} = \begin{bmatrix} \left[\tilde{\mathbf{y}}_{\text{diff}}^{\text{ULA}}\right]_{L_{ss}} & \left[\tilde{\mathbf{y}}_{\text{diff}}^{\text{ULA}}\right]_{L_{ss}-1} & \cdots & \left[\tilde{\mathbf{y}}_{\text{diff}}^{\text{ULA}}\right]_1 \\ \left[\tilde{\mathbf{y}}_{\text{diff}}^{\text{ULA}}\right]_{L_{ss}+1} & \left[\tilde{\mathbf{y}}_{\text{diff}}^{\text{ULA}}\right]_{L_{ss}} & \cdots & \left[\tilde{\mathbf{y}}_{\text{diff}}^{\text{ULA}}\right]_2 \\ \vdots & \vdots & \ddots & \vdots \\ \left[\tilde{\mathbf{y}}_{\text{diff}}^{\text{ULA}}\right]_{2L_{ss}-1} & \left[\tilde{\mathbf{y}}_{\text{diff}}^{\text{ULA}}\right]_{2L_{ss}-2} & \cdots & \left[\tilde{\mathbf{y}}_{\text{diff}}^{\text{ULA}}\right]_{L_{ss}} \end{bmatrix}. \tag{12}$$

with

$$\left[\tilde{\mathbf{y}}_{\text{diff}}^{\text{ULA}}\right]_i = \frac{1}{|\mathbb{M}(i)|}\sum_{(n_1,n_2)\in\mathbb{M}(i)}\langle\tilde{\mathbf{R}}_{\mathbf{y}}\rangle_{n_1,n_2}, \tag{13}$$

$$\mathbb{M}(i) = \{(n_1, n_2)|n_1 - n_2 = i \in \mathbf{y}_{\text{diff}}^{\text{ULA}}\}. \tag{14}$$

where $\mathbf{y}_{\text{diff}}^{\text{ULA}}$ is the contiguous part of the difference co-array constructed from $\mathbf{y}(t)$. $\langle\tilde{\mathbf{R}}_{\mathbf{y}}\rangle_{n_1,n_2}$ denotes the value of the covariance matrix $\tilde{\mathbf{R}}_{\mathbf{y}}$ at the support location n_1, n_2 [13]. The MUSIC algorithm for DOA estimation can be performed directly for DOA estimation based on (11) or (12).

3. The difference co-array on moving platform

For a fixed sparse array with K sensors, the sensors are located at

$$\mathbb{P}_x = \{nd, n \in \mathbb{S}_x\}, \tag{15}$$

where $\mathbb{S}_x$ is an integer set. The difference co-array is defined as,

$$\mathbb{D}_x = \{n_1 - n_2, n_1, n_2 \in \mathbb{S}_x\}, \tag{16}$$

The sensor positions of the shifted array after moving a half-wavelength are expressed as,

$$\mathbb{P}_t = \left\{n'd, n' \in \mathbb{S}_t\right\}, \tag{17}$$

where $\mathbb{S}_t$ is an integer set corresponding to the shifted array. The sensor positions of the synthetic array, consisting of both the original and the shifted arrays, are given by,

$$\mathbb{P}_s = \mathbb{P}_x \cup \mathbb{P}_t. \tag{18}$$

It was shown in [26] that the difference co-array of the synthetic array $\mathbb{D}_s$ consists of the difference co-array of the original array $\mathbb{D}_x$ and its unit lag shifted versions $\mathbb{D}_x^L$ and $\mathbb{D}_x^R$ along and opposite to direction of motion, respectively,

$$\mathbb{D}_s = \mathbb{D}_x \cup \mathbb{D}_x^L \cup \mathbb{D}_x^R. \tag{19}$$

An example of the original array, the shifted array, the synthetic array, the difference co-arrays of the original array, and the synthetic array is depicted in Fig. 2, where K=13. Only the non-negative part of the difference co-array is shown. It is clear that the synthetic array $\mathbb{S}_s$ has more sensors due to the combination of the $\mathbb{S}_x$ and $\mathbb{S}_t$. Concerning the difference co-array, $\mathbb{D}_x^L$ fills the left hole, whereas $\mathbb{D}_x^R$ fills the right hole which results in filling most of the holes in $\mathbb{D}_x$. Some holes remain, such as the holes 33 and 38 in Fig. 2 since only the neighboring holes of the available lags are filled,.

4. The proposed sparse array

A structured sparse array using two subarrays with different sensor spacings is proposed. From Section 3 and the work in [26], the array motion can fill the two neighboring holes of each lag. This property implies that a fully augmented sparse array can emerge from array motion when the number of consecutive holes in the difference co-array is less than 3. The array configurations of the proposed array are depicted in Fig. 3. Here, the numbers of sensors in the two subarrays assume integer values M, N. The sensor spacing of one subarray is set as $d_x d$ ($d_x = 3$), whereas the spacing for the other subarray is $d_y d$. The distance between the first sensors of the two subarrays is defined as Ld, where L is an integer. The proposed array can be divided into three categories according to L, which are depicted in Fig. 3(a)–(c). The total number of the sensors is $K \le M + N$. It is noted that M and N are not necessarily coprime integers as in the case of the coprime array or the generalized coprime array. This relaxed condition also applies to d_x and d_y.

The sensor positions of the proposed array are expressed as

$$\mathbb{P} = \{md_x d, 0 \le m \le M-1\} \cup \{(nd_y + L)d, 0 \le n \le N-1\}. \tag{20}$$

The above equation describes the configuration in Fig. 3(a) for $L = 0$.

Proposition 1: The co-array of the synthetic array of the proposed array has the following properties:

(1) It is a fully filled co-array when $d_y \le 3M$ and $L \le 6M$.

(2) The maximum DOF of the difference co-array for the various array parameters is provided in TABLE I, when $d_y = 3M$.

Proof. For the array in Fig. 3(a) and (b), i.e., $0 \le L \le 3(M-1)$, there exists at least one overlapping sensor between subarray1 and subarray2. The self-lags of the subarray1 provide all consecutive lags for its corresponding difference co-array after array motion. Therefore, the difference co-array of the synthetic array is a hole-free array only when the difference of the neighboring lags of the cross-lags between the subarray1 and subarray2 is less than 3, i.e.,

$$kd_y - 3(M-1) - (k-1)d_y \le 3, \quad k \in [1, N-1], \tag{21}$$

From the above equation, $d_y \le 3M$. For $3(M-1) < L \le 6M$, the cross-lag between the last sensor of subarray1 and the first sensor of subarray2 should satisfy the following expression, in addition to condition $d_y \le 3M$ (Table 1).

$$L - 3(M-1) - 3M \le 3. \tag{22}$$

which yields $L \le 6M$, and this proves the first property.

Regarding the proof of the second property, we start from $L = 0$. The maximum DOF is equivalent to the maximum array aperture due to the existence of the hole-free difference co-array. For $d_y > 3(M-1)$, the position of the second sensor in subarray2 is greater than that of the last sensor in subarray1. This results in the

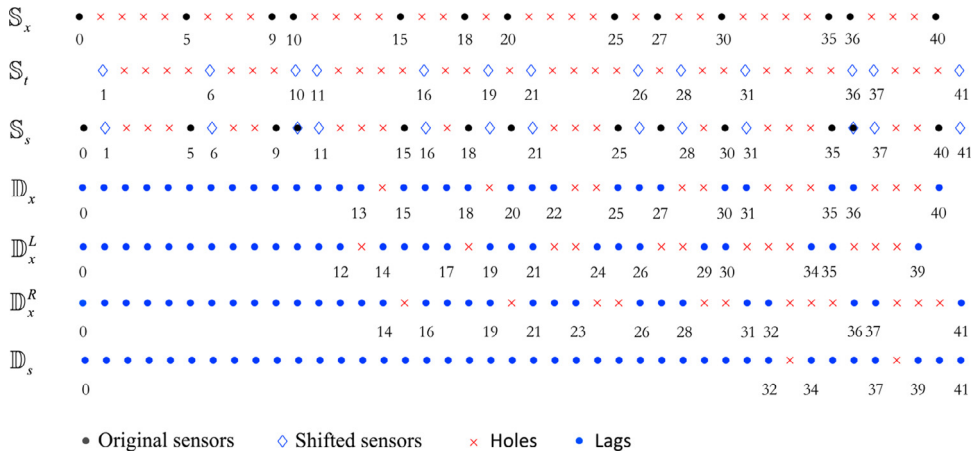

Fig. 2. An example of the original array, the shifted array, the synthetic array, the difference co-arrays of the original array and the synthetic array, where K=13.

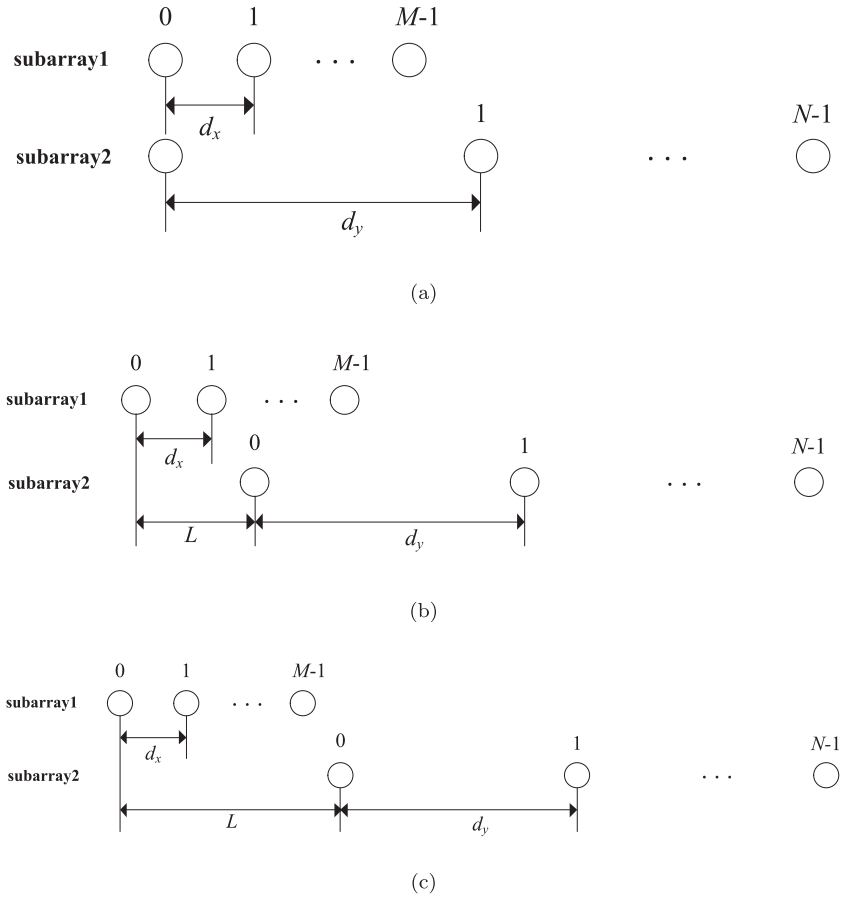

Fig. 3. Configurations of the proposed array. (a) L=0; (b) $0 < L \leq 3(M-1)$; (c) $3(M-1) < L \leq 6M$.

Table 1
Parameters for the maximum DOF of the synthetic array.

L	K	K is odd or even	M, N	$\text{DOF}_{\max}$
$L=0$	$K=M+N-1$	odd	$M=N=\frac{K+1}{2}$ or $M=\frac{K-1}{2}, N=\frac{K+3}{2}$	$\frac{3(K^2-1)}{4}+2$
		even	$M=\frac{K}{2}, N=\frac{K}{2}+1$	$\frac{3K^2}{4}+2$
$L=3(M-1)$	$K=M+N-1$	odd	$M=N=\frac{K+1}{2}$	$\frac{3(K-1)(K+3)}{4}+2$
		even	$M=\frac{K}{2}, N=\frac{K}{2}+1$ or $M=\frac{K}{2}+1, N=\frac{K}{2}$	$\frac{3(K^2+2K)}{4}-1$
$L=6M$	$K=M+N$	odd	$M=\frac{K+1}{2}, N=\frac{K-1}{2}$	$\frac{3(K+1)^2}{4}+2$
		even	$M=N=\frac{K}{2}$, or $M=\frac{K}{2}+1, N=\frac{K}{2}-1$	$\frac{3K(K+2)}{4}+2$

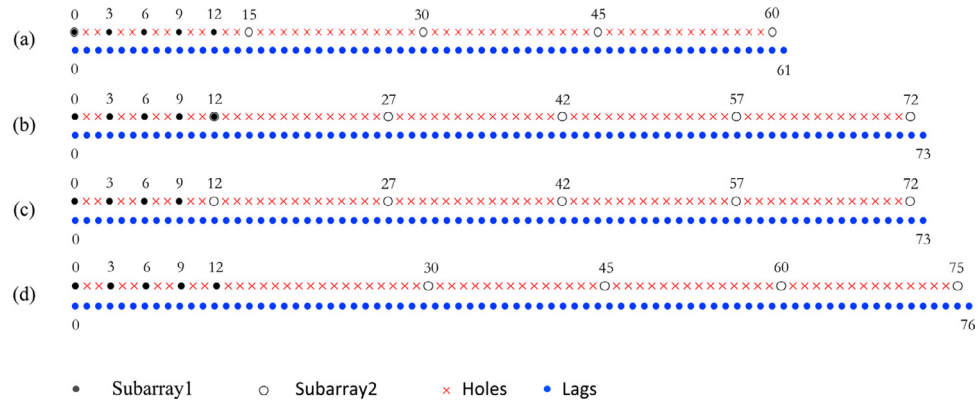

Fig. 4. An example of the proposed array and the dilated nested array, where K=9 and $d_y = 3M$. (a) $L = 0, M = N = 5$; (b) $L = 3(M-1),\ M = N = 5$; (c) the dilated nested array, $N_1 = 4, N_2 = 5$; (d)$L = 6M,\ M = 5, N = 4$.

existence of only one overlapping sensor between subarray1 and subarray2, which can be seen from Fig. 3(a), i.e., $K = M + N - 1$. Therefore, the DOF of the synthetic array can be expressed as $\text{DOF} = (N-1)d_y + 2$. The constant, 2, is the sum of the zero-lag and the additional lag due to array motion. The maximum DOF is denoted as $\text{DOF}_{\max} = 3M(N-1) + 2$ since $d_y \le 3M$. Substituting $K = M + N - 1$ into $\text{DOF}_{\max} = 3M(N-1) + 2$, we obtain $\text{DOF}_{\max} = 3M(K-M) + 2$. The expressions in TABLE I for $L = 0$ can be obtained by maximizing the function $\text{DOF}_{\max}$. For $0 < L \le 3(M-1)$, $\text{DOF} = L + (N-1)d_y + 2$. The upper bound $\text{DOF}_{\max} = 3(M-1) + 3M(N-1) + 2$ corresponds to $L = 3(M-1)$. Similarly, $\text{DOF}_{\max}$ can be expressed as the function of K to solve for the optimal M, N. It is noted that $K = M + N$ for $3(M-1) < L \le 6M$ since there are no overlapping sensors between the two subarrays (see Fig. 3(c)). Similar to $0 < L \le 3(M-1)$, $\text{DOF}_{\max} = 6M + 3M(N-1) + 2$ for $L = 6M$. The maximum DOF and the optimal M, N can be obtained by substituting $K = M + N$ into $\text{DOF}_{\max} = 6M + 3M(N-1) + 2$. The proof is complete. □

An example is shown in Fig. 4, where the sensor positions and the difference co-arrays of the synthetic array are depicted for $L = 0$ (see Fig. 4(a)), $L = 3M - 1$ (see Fig. 4(b)) and $L = 6M$ (see Fig. 4(d)) when $K = 9$ and $d_y = 3M$. We set $M = N = 5$ for Fig. 4(a) and (b), and $M = 5, N = 4$ for Fig. 4(d). It is evident that all the aforementioned difference co-arrays of synthetic array are fully filled. The case of Fig. 4(d) offers the highest DOF since there are no overlapping sensors between the two subarrays.

4.1. Bounds on nested arrays

The nested array, on fixed platforms, consisting of two uniform subarrays and producing a hole-free difference co-array, was given in [5], where one subarray has a unit sensor spacing. The concept of the nested array was extended in [11] and [28] by the means of compression or dilation of the sensor spacing. In this paper, we propose to enhance the DOF in sparse arrays on moving platform by compressing the sensor spacing of one subarray and dilating that of the other. For $L = 0$, the proposed array is a nested array when $3(M-1) \le d_y \le 3M$. However, it is worthy noting that it is not an optimum configuration since the first sensors of the two subarrays coincide in positions, which leads to a decrease in the array aperture. This can be seen in Fig. 4(a) and (c), where $K = 9, N_1 = 4, N_2 = 5$ for the dilated nested array. The proposed array deviates from a nested array for $d_y < 3(M-1)$, but it is still a sparse array whose difference co-array is fully filled. The condition on this deviation is $L + d_y < 3(M-1)$ for $0 < L \le 3(M-1)$. The proposed array has the same array configuration as the dilated nested array for $L = 3(M-1)$, which can be seen in Fig. 4(b) and (c). It becomes a nested array for $3(M-1) < L \le 6M$. Although it has the similar array configuration as the dilated nested array, the proposed array structure has a higher DOF since the distance between the last sensor of subarray1 and the first sensor of subarray2 is increased, which can be observed in Fig. 4(c) and (d).

4.2. The non-coprimality of the proposed array

In some situations, the non-coprimality of the proposed array offers higher DOF than coprimality. Considering the first case of Fig. 3, the maximum DOF of a synthetic non-nested array is $\text{DOF}_{\max} = (3M-4)(N-1) + 2$ for $d_y = 3M - 4$, according to the conclusion of last subsection. The optimal M, N are obtained by maximizing the quadratic function $\text{DOF}_{\max} = (3M-4)(K-M) + 2$, where $K = M + N - 1$. The solution is denoted as $M = round(K/2 + 2/3), N = round(K/2 + 1/3)$, where $round(x)$ rounds each element of x to the nearest integer. For instance, 46 non-negative lags are obtained when $M = N = 5$ for $K = 9$, as depicted in Fig. 5(a), whereas 42 non-negative lags for $M = 4, N = 6$ in Fig. 5(b). When the coprime integers are $M = 3, N = 7$, then 32 non-negative lags are produced, as shown in Fig. 5(c). They represent non-nested arrays, while the coprimality of M, N offers least DOF.

5. Simulation results

In this section, we examine the DOA estimation performance of the proposed array structure using the MUSIC pseudo spectrum and the root mean-square error (RMSE), defined as

$$\text{RMSE} = \sqrt{\frac{1}{QN_m}\sum_{p=1}^{N_m}\sum_{q=1}^{Q}\left(\hat{\theta}_q(p) - \theta_q\right)^2}, \tag{23}$$

where $\hat{\theta}_q(p)$ is the estimate of the source angle θ_q obtained from the pth Monte Carlo trial. N_m is the number of Monte Carlo trials.

5.1. DOA estimation

In the first simulation, we examine the MUSIC spectra based on the proposed array with the maximum DOF. We assume $K = 9$, $d_y = 3M$, and Q sources distributed uniformly over $d\sin\theta/\lambda = [-0.49, 0.49]$. We use 1,000 snapshots. The input signal-to-noise ratio (SNR) is set to 10 dB. The different values of $L = 0$, $L = 3(M-1)$ and $L = 6M$ are considered, with the corresponding numbers $M = N = 5$, $M = N = 5$ and $M = 5, N = 4$, respectively. The respective numbers of sources Q are 58, 68 and 72. The co-array MUSIC in [13] is applied, and the corresponding MUSIC spectra are shown in Fig. 6. It is evident that all the sources are distinguished,

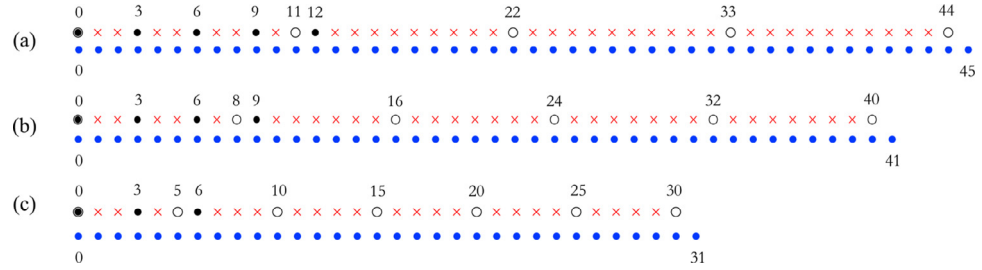

Fig. 5. An example of the non-coprimality of the proposed array, where K=9, $L=0$ and $d_y=3M-4$. (a) $M=N=5$; (b) $M=4, N=6$; (c)$M=3, N=7$.

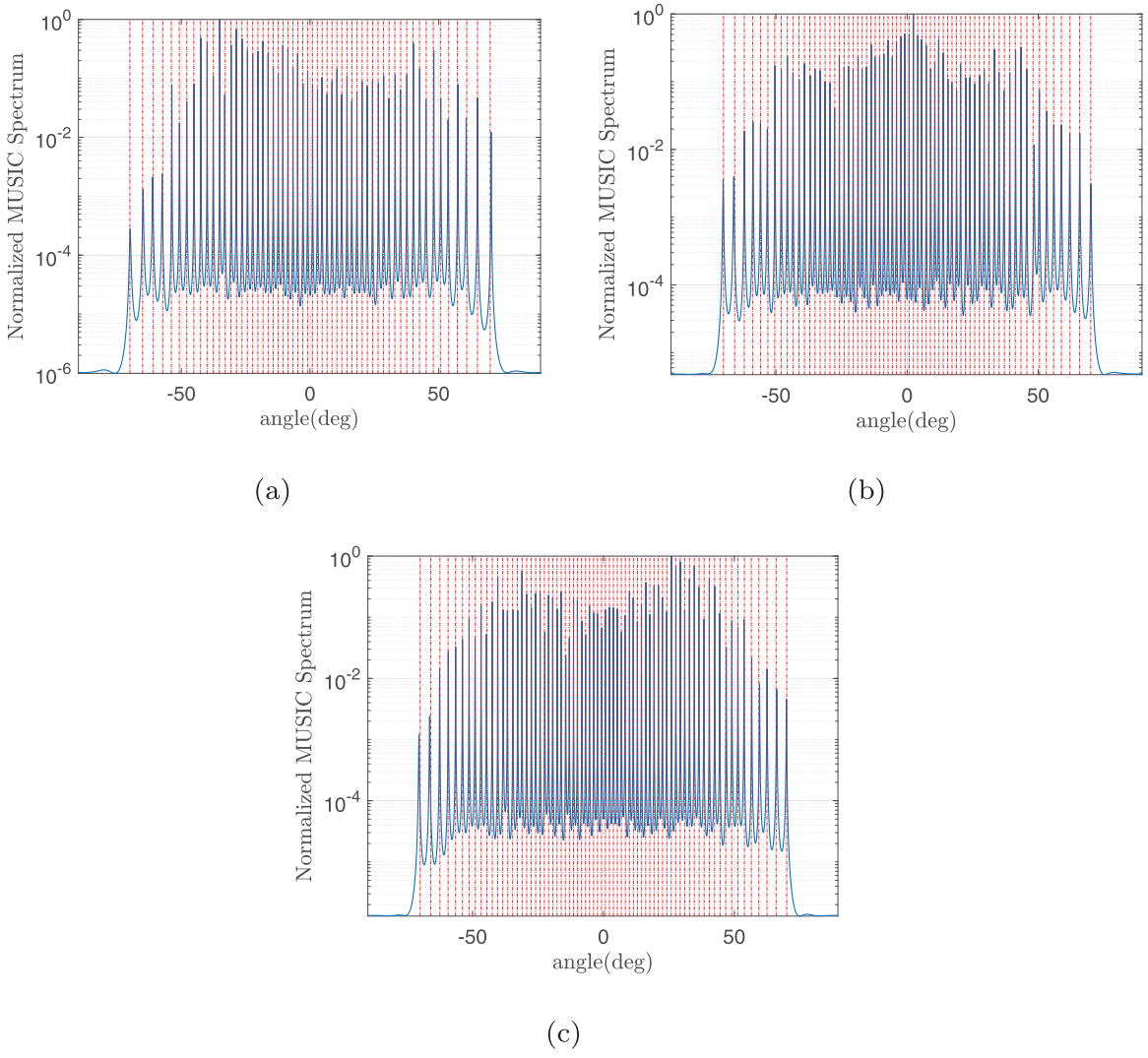

Fig. 6. MUSIC spectra using the maximum DOF of the proposed array, where K=9 and $d_y=3M$. (a) $L=0, M=N=5, Q=58$; (b) $L=3(M-1),\ M=N=5,\ Q=68$; (c) $L=6M,\ M=5, N=4, Q=72$.

which is rather expected since the synthetic array of the proposed array can offer 61, 73 and 75 consecutive lags, respectively.

In the second simulation example, we examine the performance of the proposed array with the non-coprimality. We set $L=0$, $K=9$, $d_y=3M-4$ and $Q=35$. Three groups of M, N are considered, namely $M=N=5$, $M=4, N=6$ and $M=3, N=7$. The third group is coprime. The other parameters are the same as the first simulation. The MUSIC spectra are shown in Fig. 7. The coprime parameters cannot identity all sources because they only provide 32 consecutive lags after array motion.

5.2. DOA estimation performance

The RMSE performance are plotted versus SNR and the number of snapshots in Figs. 8 and 9, respectively, where different values of L, M, N and d_y of the proposed array are used. $Q=25$ uncorrelated sources for $K=9$ are used to guarantee the number of sources to be lower than the available DOFs for all cases. 200 independent trails are used in all simulations. In Fig. 8, 500 snapshots of data are utilized and the input SNR varies between -10 dB and 20 dB. All curves decrease in values with SNR increments. The array with the parameters of $M=5$, $N=4$, $L=6M$ and $d_y=3M$ be-

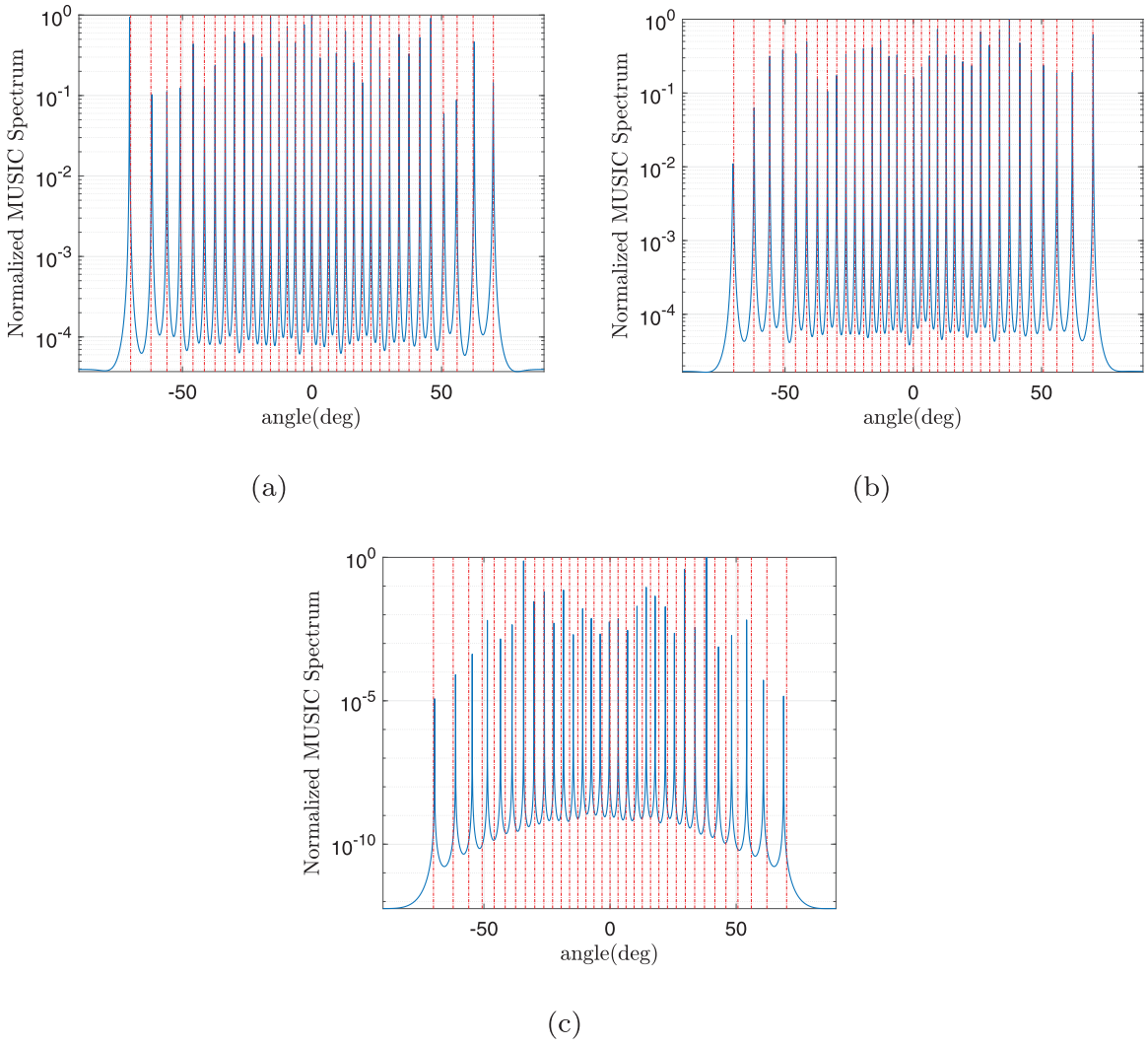

Fig. 7. MUSIC spectra using the non-coprimality of the proposed array, where K=9, $L=0$, $Q=35$ and $d_y=3M-4$. (a) $M=N=5$; (b) $M=4, N=6$; (c)$M=3, N=7$.

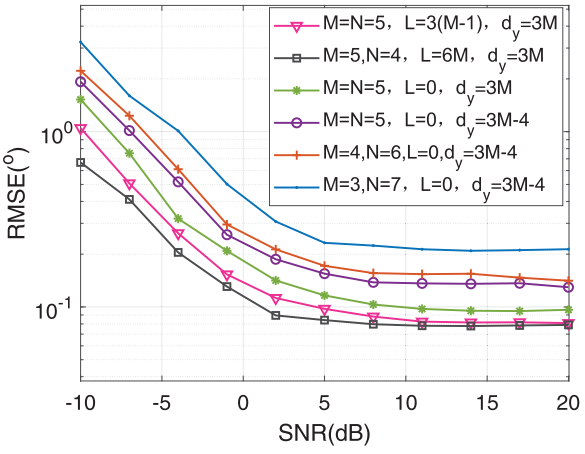

Fig. 8. RMSE vs. input SNR.

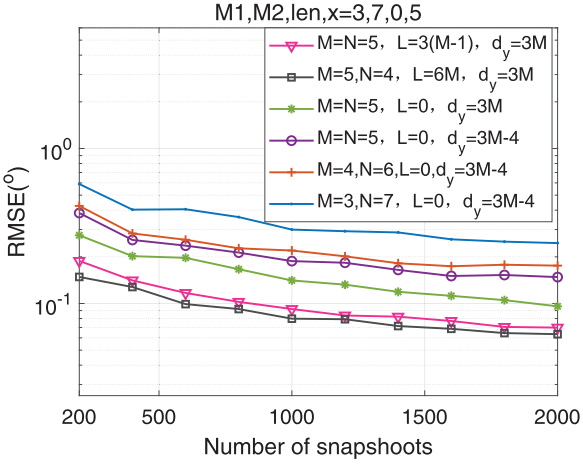

Fig. 9. RMSE vs. the number of snapshots.

haves the best in all cases, while the coprime $M=3, N=7$ with the parameters $L=0$ and $d_y=3M-4$ performs the worst. This is because the former has the maximum DOFs in the difference co-array, whereas the coprime case offers the minimum DOFs. It is noted that there are no overlapping sensors between the two sub-arrays for the former case, which leads to $M=5,\ N=4$. In Fig. 9, we set SNR equal to 0 dB and vary the number of snapshots from 200 to 2000. Clearly, similar results regarding the superiority of the performance of the proposed array can be observed from the figure.

6. Conclusion

A sparse array design for moving platforms was proposed. The array utilizes two uniform subarrays to construct a fully filled difference co-array which can estimate a number of sources largely exceeding the number of sensors. The sensor spacings of the two subarrays were such as the neighboring sensors of one subarray of M sensors are separated by three times the unit spacing while those in the other subarray of N sensors are separated by no more than $3M$. The nested array emerges as a special case of the proposed array when the array parameters satisfy certain conditions. The non-coprimality of M, N is shown to be better than coprimality in the case where the two subarrays share the reference sensor. The analysis and simulations presented in this paper assume accurate platform velocity knowledge and no sensor position perturbations.

Declaration of Competing Interest

We declare that we have no financial and personal relationships with other people or organizations that can inappropriately influence our work; there is no professional or other personal interest of any nature or kind in any product, service and/or company that could be construed as influencing the position presented in, or the review of, the manuscript submitted.

References

[1] P. Stoica, Z. Wang, J. Li, Extended derivations of MUSIC in the presence of steering vector errors, IEEE Trans. Signal Process. 53 (3) (2005) 1209–1211, doi:10.1109/TSP.2004.842201.

[2] X. Yuan, Coherent source direction-finding using a sparsely-distributed acoustic vector-sensor array, IEEE Trans. Aerosp. Electron. Syst. 48 (3) (2012) 2710–2715, doi:10.1109/TAES.2012.6237621.

[3] M.G. Amin, X. Wang, Y.D. Zhang, F. Ahmad, E. Aboutanios, Sparse arrays and sampling for interference mitigation and DOA estimation in GNSS, Proc. IEEE 104 (6) (2016) 1302–1317, doi:10.1109/JPROC.2016.2531582.

[4] P.P. Vaidyanathan, P. Pal, Sparse sensing with co-prime samplers and arrays, IEEE Trans. Signal Process. 59 (2) (2011) 573–586, doi:10.1109/TSP.2010.2089682.

[5] P. Pal, P.P. Vaidyanathan, Nested arrays: a novel approach to array processing with enhanced degrees of freedom, IEEE Trans. Signal Process. 58 (8) (2010) 4167–4181, doi:10.1109/TSP.2010.2049264.

[6] Y.D. Zhang, M.G. Amin, B. Himed, Sparsity-based DOA estimation using co-prime arrays, in: Proc. IEEE Int. Conf. Acoustics, Speech and Signal Process. (ICASSP), Vancouver, Canada, 2013, doi:10.1109/icassp.2013.6638403.

[7] B. Liao, S. Chan, Direction-of-arrival estimation in subarrays-based linear sparse arrays with gain/phase uncertainties, IEEE Trans. Aerosp. Electron. Syst. 49 (4) (2013) 2268–2280, doi:10.1109/TAES.2013.6621815.

[8] Z. Tan, A. Nehorai, Sparse direction of arrival estimation using co-prime arrays with off-grid targets, IEEE Signal Process. Lett. 21 (1) (2014) 26–29, doi:10.1109/LSP.2013.2289740.

[9] Y. Gu, Y.D. Zhang, N.A. Goodman, Optimized compressive sensing-based direction-of-arrival estimation in massive MIMO, in: Proc. IEEE Int. Conf. Acoustics, Speech and Signal Process. (ICASSP), New Orleans US, 2017, pp. 3181–3185, doi:10.1109/ICASSP.2017.7952743.

[10] K. Adhikari, J.R. Buck, K.E. Wage, Extending coprime sensor arrays to achieve the peak side lobe height of a full uniform linear array, EURASIP J. Adv. Signal Process. 2014 (2014:148) (2014) 1–17, doi:10.1186/1687-6180-2014-148.

[11] S. Qin, Y.D. Zhang, M.G. Amin, Generalized coprime array configurations for direction-of-arrival estimation, IEEE Trans. Signal Process. 63 (6) (2015) 1377–1390, doi:10.1109/TSP.2015.2393838.

[12] P. Pal, P.P. Vaidyanathan, Pushing the limits of sparse support recovery using correlation information, IEEE Trans. Signal Process. 63 (3) (2015) 711–726, doi:10.1109/TSP.2014.2385033.

[13] C. Liu, P.P. Vaidyanathan, Remarks on the spatial smoothing step in coarray MUSIC, IEEE Signal Process. Lett. 22 (9) (2015) 1438–1442, doi:10.1109/LSP.2015.2409153.

[14] C. Zhou, Y. Gu, Y.D. Zhang, Z. Shi, T. Jin, X. Wu, Compressive sensing-based coprime array direction-of-arrival estimation, IET Commun. 11 (11) (2017) 1719–1724, doi:10.1049/iet-com.2016.1048.

[15] M. Yang, L. Sun, X. Yuan, B. Chen, A new nested MIMO array with increased degrees of freedom and hole-free difference coarray, IEEE Signal Process. Lett. 25 (1) (2018) 40–44, doi:10.1109/LSP.2017.2766294.

[16] W. Wang, S. Ren, Z. Chen, Unified coprime array with multi-period subarrays for direction-of-arrival estimation, Digital Signal Process. 74 (2018) 30–42, doi:10.1016/j.dsp.2017.11.015.

[17] C. Zhou, Z. Shi, Y. Gu, X. Shen, DECOM: DOA estimation with combined music for coprime array, in: Proc. International Conference on Wireless Communications and Signal Processing, 2013, pp. 1–5, doi:10.1109/WCSP.2013.6677080.

[18] X. Wang, M. Amin, X. Cao, Analysis and design of optimum sparse array configurations for adaptive beamforming, IEEE Trans. Signal Process. 66 (2) (2018) 340–351, doi:10.1109/TSP.2017.2760279.

[19] E. BouDaher, Y. Jia, F. Ahmad, M.G. Amin, Multi-frequency co-prime arrays for high-resolution direction-of-arrival estimation, IEEE Trans. Signal Process. 63 (14) (2015) 3797–3808, doi:10.1109/TSP.2015.2432734.

[20] C. Zhou, Y. Gu, X. Fan, Z. Shi, G. Mao, Y.D. Zhang, Direction-of-arrival estimation for coprime array via virtual array interpolation, IEEE Trans. Signal Process. 66 (22) (2018) 5956–5971, doi:10.1109/TSP.2018.2872012.

[21] C. Zhou, Y. Gu, Z. Shi, Y.D. Zhang, Off-grid direction-of-arrival estimation using coprime array interpolation, IEEE Signal Process. Lett. 25 (11) (2018) 1710–1714, doi:10.1109/LSP.2018.2872400.

[22] A. Moffet, Minimum-redundancy linear arrays, IEEE Trans. Antennas Propagat. 16 (2) (1968) 172–175, doi:10.1109/TAP.1968.1139138.

[23] D.A. Linebarger, I.H. Sudborough, I.G. Tollis, Difference bases and sparse sensor arrays, IEEE Trans. Inform. Theory 39 (2) (1993) 716–721, doi:10.1109/18.212309.

[24] S.M. Alamoudi, M.A. Aldhaheri, S.A. Alawsh, A.H. Muqaibel, Sparse doa estimation based on a shifted coprime array configuration, in: 2016 16th Mediterranean Microwave Symposium (MMS), 2016, pp. 1–4, doi:10.1109/MMS.2016.7803789.

[25] J. Ramirez, J.L. Krolik, Synthetic aperture processing for passive co-prime linear sensor arrays, Digital Signal Process. 61 (2017) 62–75, doi:10.1016/j.dsp.2016.07.021.

[26] G. Qin, M.G. Amin, Y.D. Zhang, Doa estimation exploiting sparse array motions, IEEE Trans. Signal Process. 67 (11) (2019) 3013–3027, doi:10.1109/TSP.2019.2911261.

[27] G. Qin, M. G. Amin, Y. D. Zhang, Analysis of coprime arrays on moving platform, in: IEEE Int. Conf. Acoustics, Speech and Signal Process. (ICASSP), Brigton, U.K., 2019, doi:10.1109/ICASSP.2014.6854226. submitted to.

[28] G. Qin, Y.D. Zhang, M.G. Amin, DOA estimation exploiting moving dilated nested arrays, IEEE Signal Process. Lett. 26 (3) (2019) 490–494, doi:10.1109/LSP.2019.2894467.

[29] G. Qin, M.G. Amin, Optimum sparse array configuration for DOA estimation on moving platforms, Digital Signal Processing 105 (2020) 102685, doi:10.1016/j.dsp.2020.102685. Special Issue on Optimum Sparse Arrays and Sensor Placement for Environmental Sensing.

[30] S. Stergiopoulos, E.J. Sullivan, Extended towed array processing by an overlap correlator, J. Acoust. Soc. Am. 86 (1) (1989) 158–171, doi:10.1121/1.398335.

[31] L. Gan, Block compressed sensing of natural images, in: Proc. Int. Conf. Digital Signal Process.(DSP2007), 2007, pp. 403–406, doi:10.1109/ICDSP.2007.4288604.

[32] Z.Yang, L.Xie, Enhancing sparsity and resolution via reweighted atomic norm minimization, IEEE Trans. Signal Process. 64 (4) (2016) 995–1006, doi:10.1109/TSP.2015.2493987.

[33] J. Shi, G. Hu, X. Zhang, F. Sun, H. Zhou, Sparsity-based two-dimensional doa estimation for coprime array: from sum difference coarray viewpoint, IEEE Trans. Signal Process. 65 (21) (2017) 5591–5604, doi:10.1109/TSP.2017.2739105.